Biosensors and Bioelectronics 78 (2016) 106–110

Contents lists available at ScienceDirect

Biosensors and Bioelectronics

journal homepage: www.elsevier.com/locate/bios

Detection of *Neisseria meningitidis* using surface plasmon resonance based DNA biosensor

Gurpreet Kaur [a], Ayushi Paliwal [a], Monika Tomar [b], Vinay Gupta [a,*]

[a] Department of Physics and Astrophysics, University of Delhi, Delhi 110007, India
[b] Physics Department, Miranda House, University of Delhi, Delhi 110007, India

ARTICLE INFO

Article history:
Received 6 August 2015
Received in revised form
21 October 2015
Accepted 10 November 2015
Available online 11 November 2015

Keywords:
Surface plasmon resonance
Neisseria meningitidis
Zinc oxide
Biosensor

ABSTRACT

Herein, we report the development of a surface plasmon resonance (SPR) based biosensor for the detection of *Neisseria meningitidis* DNA employing Kretschmann configuration. Highly *c*-axis oriented ZnO thin film of thickness 200 nm was deposited on gold coated glass prisms by RF sputtering technique. Single stranded probe DNA was immobilized on the surface of ZnO thin film by physical adsorption method. SPR reflectance curves were recorded as a function of incident angle of He–Ne laser beam using a laboratory assembled SPR setup. The prepared biosensor exhibits a linear response towards target meningitidis DNA over the concentration range from 10 to 180 ng/μl with a high sensitivity of about 0.03°/(ng/μl) and a low limit of detection of 5 ng/μl. The SPR biosensor demonstrated high specificity and long shelf life thus, pointing towards a promising application in the field of meningitidis diagnosis.

1. Introduction

Neisseria meningitidis (*N. meningitidis*) is a pathogen which is the root cause of bacterial meningitis globally. Bacterial meningitis is a grave infection of the meninges (outer membrane) of the brain and spinal cord which can even lead to death (Schneider et al., 2007). It is highly infectious and can spread rapidly through contact. Moreover, the symptoms of meningitis are similar to that of common flu. Hence, rapid and sensitive diagnosis of the disease is crucial for prevention and control of epidemic (Dash et al., 2013). Conventional techniques for meningitis detection include Polymerase chain reaction (PCR), Real time-PCR, microarray and latex agglutination test (Zhu et al., 2012; Chiba et al., 2009; Wang et al., 2012; Surinder et al., 2007; Ben et al., 2008). However, these techniques are time consuming and less sensitive. To improve the turnaround time, a few attempts have been made to develop electrochemical DNA biosensors for detection of *N. meningitidis* (Tak et al., 2014; Dash et al., 2014; Patel et al., 2010, 2009). It is important to point out that these electrochemical biosensors require an external redox probe for detection. Moreover, they rely on the transfer of electrons from the redox center of the probe to the electrode. This indirect way of detection is prone to hindrances in the charge flow path which may hamper its calibration. On the other hand, optical DNA biosensors rely on the change in optical parameters (absorption, refractive index etc.) instead of charge transfer. Besides, any external artificial redox agent is not required in this case. It may be noted that the label-free and reliable optical biosensing has not been reported for meningitis detection yet.

Surface plasmon resonance (SPR), an optical biosensing technique, is a powerful, highly sensitive and label-free tool for studying biomolecular interactions (Homola, 2008). SPR based biosensors employ surface plasmon polaritons to probe the interactions occurring at the sensor surface by monitoring the change in refractive index. An incident light excites surface plasmons at the metal–dielectric interface and any variation in the medium's properties changes its propagation constant (Zhang et al., 2012, 2013; Špringer and Homola, 2012). SPR based biosensors score over electrochemical biosensors since they provide fast and label-free detection of biomolecules directly (Arya et al., 2007). Besides, SPR biosensors offer a higher sensitivity as the fine variations occurring in the vicinity of the matrix (dielectric) due to biochemical reaction will change the refractive index and hence, the characteristics of the surface plasmon wave. As a result, they have been employed for the detection of various biological analytes including DNA (Helmerhorst et al., 2012).

The SPR based DNA biosensors are based on monitoring of DNA hybridization. Hence, the sensitivity of the biosensor relies on the interaction between the immobilized probe DNA and its complementary target sequence. Selection of an appropriate matrix plays a crucial role in fabrication of an efficient biosensor. In this context, metal oxide nanostructures provide an efficient platform for effective immobilization of biomolecules. Among various metal oxides, Zinc oxide (ZnO) nanostructures have captivated the interest of researchers owing to their good biocompatibility, high

* Corresponding author.
E-mail address: drguptavinay@gmail.com (V. Gupta).

http://dx.doi.org/10.1016/j.bios.2015.11.025
0956-5663/

chemical stability, ease of fabrication, high isoelectric point and high surface to volume ratio (Liu et al., 2013; Israr et al., 2011; Das et al., 2010). Thus, ZnO is a suitable platform for immobilization of biomolecules as the biomolecules immobilized on ZnO are known to retain their conformational orientation which warrants retention of their biocompatibility.

Limited work has been carried out on ZnO/Au based SPR biosensors for various analytes. Wang et al. reported a ZnO–Au nanocomposite for detection of immunoglobulin protein. However, their experiment was based on wavelength interrogation while the present manuscript focuses on angular interrogation method. Further, they employed a complicated ZnO–Au-protein probe immobilized using covalent binding by functionalizing the nanocomposite (Wang et al. 2009, 2010). Chang et al. utilized angular interrogation method for detection of CA 15-3 but they deposited Au layer on top of ZnO thin film thus, using Au as the immobilization matrix. So, the surface had to be functionalized involving a long rigorous procedure which resulted in a lesser amount of shift in the SPR angle (Chang et al., 2010). The only report on ZnO/Au system for DNA detection using SPR suffered from stability problems. Byun et al. deposited ZnO thin film using chemical route even though sputtering method allows accurate thickness control along with excellent stability and reproducibility. This resulted in poor stability owing to which they had to rinse the chip in order to decrease the ZnO solubility in buffer and have not mentioned about the shelf life of the biosensor (Byun et al., 2011).

The present work is an endeavor to detect *N. meningitidis* DNA using laboratory assembled SPR technique. ZnO thin film has been deposited on gold coated glass prisms by RF sputtering. Single stranded probe DNA (ssDNA) was immobilized on its surface. DNA hybridization on the surface of the sensor leads to a change in optical properties at Au–ZnO interface. Thus, a continuous shift in the SPR reflectance and hence, in the dip angle is observed with increase in concentration of target DNA. This is the first report on SPR based *N. meningitidis* biosensor to the best of our knowledge.

2. Experimental

N. meningitidis oligonucleotides were purchased from Sigma-Aldrich. Tris buffer and ethylene diamine tetra acetic acid (EDTA) were procured from Sisco chemicals, India. All oligonucleotide solutions of varying concentrations were prepared in Tris–EDTA (TE) buffer (10 mM Tris, pH 8.0, 1 mM EDTA). The oligonucleotide sequences used in the present study are as follows:

Probe DNA: 5′-HS-GATACGAATGTGCAGCTGACACG-3′

Complementary target DNA: 5′-CGTGTCAGCTGCACATTCGTATC-3′

Non-complementary DNA 1: 5′-GCACACACGTGGTCAAACGA TTC-3′

Non-complementary DNA 2: 5′-TAAAGCATTCCTAGCTAG-GAATC-3′

Gold thin film of 40 nm thickness was deposited on the BK-7 glass prism (Au/prism) using thermal evaporation technique. The gold coated prisms were annealed in air at 250 °C for 1 h. ZnO film (200 nm thin) was deposited on the Au/prism (ZnO/Au/prism) using Zn metal target (99.999% pure) by RF magnetron sputtering technique. The film was deposited in mixed argon and oxygen ambient at a substrate temperature of 250 °C. The typical deposition parameters are reported elsewhere (Paliwal et al., 2014).

Surface Plasmon Resonance of the air/ZnO/Au/prism system has been studied in the Kretschmann configuration using an indigenously developed SPR setup. The laboratory assembled system consists of p-polarized He–Ne laser (wavelength = 633 nm), a prism table and a photodetector. The prism table is attached to a micro-controlled stepper motor driven stage which can be moved in *X*, *Y* and *Z* directions and rotated about its own axis with accuracy of 0.03°. The Si photodetector is attached to a high resolution power meter (Newport 1936-R) for reflectance measurements. SPR studies were carried out using this system and the reflected light intensity of laser beam was measured as a function of incident angle.

ZnO has a high isoelectric point (~9.5) as compared to DNA (~4.5) and thus, behaves as a positively charged entity at neutral pH. Hence, the immobilization of DNA on the surface of ZnO thin film takes place via electrostatic interaction. 10 µl of single stranded DNA probe solution (5 ng/µl) was immobilized on the ZnO/Au/prism (ssDNA/ZnO/Au/prism) using physical adsorption technique and incubated at 25 °C for 3 h. The prism was washed with TE buffer to remove unbound DNA and dried. For hybridization, the prepared system (ssDNA/ZnO/Au/prism) was incubated with the complementary DNA sequence at the same temperature for an optimized time of 35 s. A schematic of the experimental process is shown in Supplementary Fig. 1.

For structural and optical characterizations, ZnO and Au thin films were deposited on BK7 glass and silicon substrates under similar growth conditions. Crystallographic structure was studied using X-ray diffraction (XRD) (Bruker D8) in θ–2θ mode. Scanning electron microscope (SEM) (Tescan MIRA 3) and Atomic Force Microscope (AFM) (Bruker Dimension Icon) were also used to examine the surface morphology of the deposited films. Fourier transform infrared spectroscopy (FTIR) (Perkin Elmer) was used to analyze the optical properties of films and also to confirm the immobilization of ssDNA. The thickness of the films was measured using surface profiler (Dektak Veeco 150).

3. Results and discussion

The XRD pattern of the ZnO/Au film deposited on glass substrate is shown is Fig. 1. The XRD peak at $2\theta = 34.10°$ corresponds to (002) plane of the hexagonal wurtzite structure of ZnO and is in agreement with reported values, indicating the growth of *c*-axis oriented ZnO thin film (Gupta and Mansingh, 1996). The appearance of other two XRD peaks at 38.01° and 44.16° in Fig. 1 is attributed to (111) and (200) planes of the underneath face-centered cubic gold structure. The crystallite size was calculated using Scherrer equation and was found to be about 19 nm for ZnO thin

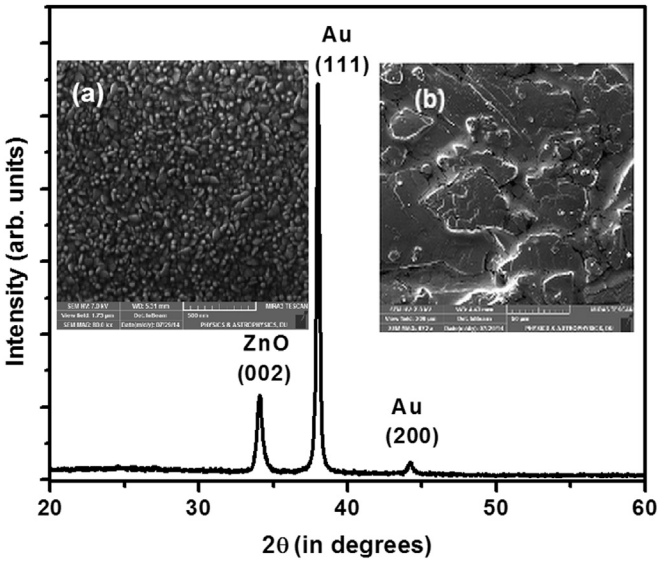

Fig. 1. XRD pattern of ZnO/Au thin film structure on glass substrate. The inset shows SEM images of (a) ZnO/Au and (b) ssDNA/ZnO/Au structures.

film and about 41 nm for Au layer.

The surface morphology of ZnO/Au/glass structure was investigated before and after DNA immobilization using SEM and obtained microimages are shown in inset of Fig. 1. A fine morphology of ZnO thin film having uniformly distributed nanosized particles can be seen (Inset: Fig. 1(a)). However, after immobilization of the ssDNA, the ZnO grains are masked by the granular structure of ssDNA layer (Inset: Fig. 1(b)). The surface of ssDNA/ZnO/Au was found to be very rough and seems to be advantageous for biosensing application (Zhou et al., 2012). The AFM image of the ZnO/Au structure is shown in Supplementary Fig. 2 which reveals the porous and nanostructured morphology of the film.

The optical properties of the ZnO/Au thin film structure deposited on Si substrate was studied using FTIR spectroscopy before and after DNA immobilization to further ascertain the immobilization of DNA, and the corresponding FTIR spectra are shown in Supplementary Fig. 3. In the FTIR spectra of ZnO/Au structure, strong and sharp characteristic peaks at 420 cm^{-1} and 570 cm^{-1} can be seen (Supplementary Fig. 3(a)) which are attributed to the vibrations of the Zn–O bond (Batra et al., 2013). Two weak absorption modes at 845 cm^{-1} and 1090 cm^{-1} are also observed in Supplementary Fig. 3(a) which might be due to the presence of some carbonate moieties or other organic compounds and are reported when FTIR samples are measured in air (Umar et al., 2009). After DNA immobilization, additional absorption peaks were observed at 1499 cm^{-1}, 1608 cm^{-1} and 1715 cm^{-1} (Supplementary Fig. 3(b)) corresponding to cytosine, adenine and guanine respectively (Ghanbari et al., 2008), confirming the successful immobilization of ssDNA on the surface of ZnO/Au structure.

The SPR reflectance curves for air/Au/prism, air/ZnO/Au/prism and air/ssDNA/ZnO/Au/prism systems are shown in Fig. 2. A sharp SPR curve for air/Au/prism system is obtained and is in agreement with the corresponding reports (Zhang et al., 2007). The reflected intensity was found to decrease rapidly with increase in incident angle of light, attaining minima (SPR dip) at a resonance angle θ_{SPR} =43.54° (Wood et al., 2013). The reflectance increased with further increase in incident angle and tended towards saturation (Fig. 2). The dotted lines in Fig. 2 correspond to experimental points whereas the solid lines represent theoretical curves which are obtained using fitting of the experimental data using Fresnel's equations for one layer (air/Au/prism), two layer (air/ZnO/Au/prism) and three layer (air/ssDNA/ZnO/Au/prism) systems respectively (Paliwal et al., 2014). A shift in the SPR curve and the resonant angle (θ_{SPR}) is observed from 43.54° to 46.59° when ZnO film is deposited on the Au/prism system, and is due to change in dielectric medium in the vicinity of Au layer. The SPR occurs at the air–Au interface in the former case (air/Au/prism) and at ZnO–Au interface in the latter (air/ZnO/Au/prism). The thickness of ZnO thin film was optimized initially before carrying out the biosensing studies. The SPR reflectance spectra were found to change significantly with varying thickness of the ZnO thin film. Since 200 nm thin ZnO film exhibited a sharp SPR reflectance curve with minimum value of reflectance at SPR angle, the same optimized film has been utilized for further study on the detection of meningitis. Upon immobilization of the single stranded DNA on the ZnO/Au/prism system, the θ_{SPR} further increased to 51.29° due to change in refractive index at the surface. It is also important to note from Fig. 2 that the value of minimum reflectance (R_{min}) at θ_{SPR} decreases significantly due to the presence of DNA molecules.

The detection of *N. meningitidis* DNA was carried out by SPR technique using prepared ssDNA/ZnO/Au/prism system. Fig. 3 illustrates the change in SPR curves upon hybridization of the ssDNA/ZnO/Au/prism with the complementary target DNA. Various concentrations of complementary DNA sequence were used and the corresponding reflectance spectra were recorded. As the concentration of target DNA was varied from 10 to 180 ng/μl, a continuous shift in the SPR reflectance curve is observed towards higher angle (Fig. 3). The observed shift in SPR curve is due to the change in the dielectric properties of ZnO matrix owing to the interaction between complementary DNA strands. Moreover, a continuous decrease in the value of R_{min} with increase in oligonucleotide concentration is also observed (Fig. 3), which further demonstrates the binding between the probe and target DNA. The hybridization of the complimentary DNA strands leads to a change in refractive index resulting in change in the angle as well as intensity of the reflected light. When surface plasmon wave (SPW) propagates at the metal–dielectric interface, the electromagnetic field of SPW extends into the dielectric medium in contact with the metal surface. The change in the optical properties in terms of refractive index leads to the change in propagation constant of the SPW. This leads to a change in the resonance conditions of SPW interacting with incident light resulting in the shift in SPR angle.

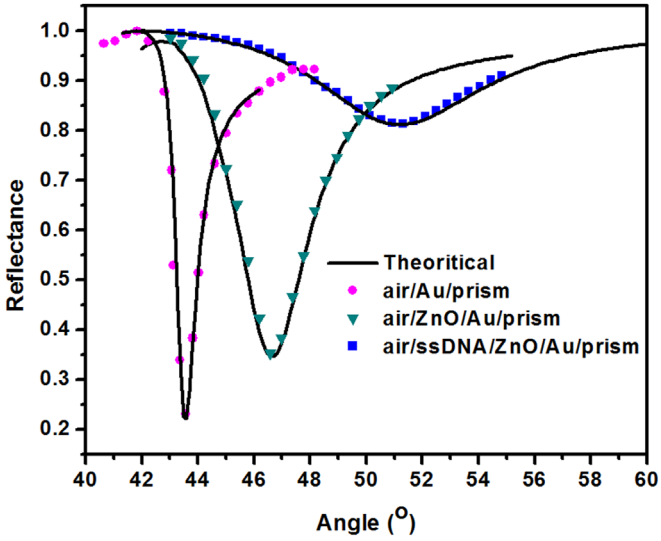

Fig. 2. SPR reflectance curves for air/Au/prism, air/ZnO/Au/prism and air/ssDNA/ZnO/Au/prism systems.

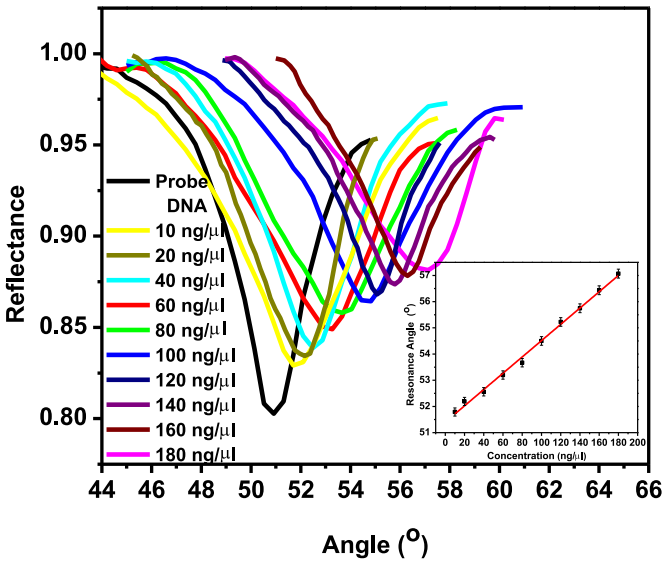

Fig. 3. SPR curves for air/ssDNA/ZnO/Au/prism system upon hybridization with different concentrations of complementary DNA. The corresponding SPR curve for probe DNA is also included for comparison. (Inset: Calibration curve for ssDNA/ZnO/Au/prism SPR biosensor).

The changes in the vicinity of metal layer may also lead to the damping of SPW and hence giving a higher value of minimum reflectance. Upon increasing the concentration of target DNA, more and more hybridization sites of the probe DNA get occupied. This results in the increase in damping due to reduction in back-scattered field and a continuous increase in the value of minimum reflectance is observed (Raether, 1986). Thus, interaction of probe DNA with increasing concentration of target DNA results in both a continuous shift in SPR angle towards higher angle and an increase in the value of minimum reflectance. The dependence of the SPR angle and the reflectance on the dielectric constant can be understood from the Fresnel's equations (Paliwal et al., 2014).

The reflectance at an incident angle θ for a single layer system (air/Au/Prism) having bare Au film of thickness d_1 is given by –

$$R_{015} = \left| \frac{r_{01} r_{15} \exp(2ik_{z1}d_1)}{1 + r_{01} r_{15} \exp(2ik_{z1}d_1)} \right|^2$$

$$r_{ik} = \frac{\left(\frac{k_{zi}}{\epsilon_i} - \frac{k_{zk}}{\epsilon_k}\right)}{\left(\frac{k_{zi}}{\epsilon_i} + \frac{k_{zk}}{\epsilon_k}\right)}$$

$$\text{and} \quad k_{zi} = \sqrt{\frac{2\pi}{\lambda}\left(\epsilon_i - \epsilon_0 \sin^2\theta\right)}$$

where ε_i with i=0, 1, 2 and 5 are the dielectric constants of the glass prism, Au film and air, respectively, and λ is the wavelength of incident light.

For a two layer system (air/ZnO/Au/prism) with ZnO layer of thickness d_2 over the Au film, the Fresnel's equation is

$$R_{0125} = \left| \frac{r_{01} + r_{125} \exp(2ik_{z1}d_1)}{1 + r_{01} r_{125} \exp(2ik_{z1}d_1)} \right|^2$$

$$\text{where } r_{125} = \frac{r_{12} + r_{25} \exp(2ik_{z2}d_2)}{1 + r_{12} r_{25} \exp(2ik_{z2}d_2)}$$

For a three layer system (air/ssDNA/ZnO/Au/prism) having immobilized probe DNA, the Fresnel's equation is modified as

$$R_{01235} = \left| \frac{r_{01} + r_{1235} \exp(2ik_{z1}d_1)}{1 + r_{01} r_{1235} \exp(2ik_{z1}d_1)} \right|^2$$

$$\text{where} \quad r_{1235} = \frac{r_{12} + r_{235} \exp(2ik_{z2}d_2)}{1 + r_{12} r_{235} \exp(2ik_{z2}d_2)}$$

Similarly, when hybridization takes place, the Fresnel's equation for a four layer system becomes

$$R_{012345} = \left| \frac{r_{01} + r_{12345} \exp(2ik_{z1}d_1)}{1 + r_{01} r_{12345} \exp(2ik_{z1}d_1)} \right|^2$$

$$\text{where} \quad r_{12345} = \frac{r_{12} + r_{2345} \exp(2ik_{z2}d_2)}{1 + r_{12} r_{2345} \exp(2ik_{z2}d_2)}$$

where subscript 0, 1, 2, 3, 4, 5 represents the different media namely prism, Au layer, ZnO film, probe DNA, target DNA and air respectively.

Thus, the change in dielectric properties of the medium will lead to a shift in the resonance angle as well as minimum reflectance.

The change in θ_{SPR} with concentration of target DNA could be plotted as the calibration curve (Inset: Fig. 3). A linear increase in the value of θ_{SPR} from 51.73° to 57.13° with increase in the concentration of target DNA from 10 to 180 ng/μl is observed in the calibration curve (Inset: Fig. 3). The prepared biosensor exhibits excellent linearity (10–180 ng/μl) with a correlation coefficient of 0.996. The sensitivity calculated from the slope of the calibration curve was about 0.03°/(ng/μl). The lower detection limit of biosensor was calculated as 3 SD/sensitivity, where SD is the standard deviation and was found to be 5 ng/μl. The detection limit of 5 ng/μL ($\sim 6 \times 10^2$ nM) and wide linear range of detection (10–180 ng/μL) as observed in the present work using ZnO nanostructured matrix is better or similar to other reports based on meningitis detection using other techniques. However, SPR has additional advantages over other techniques as discussed earlier. Till date, no report is available on the detection of meningitis DNA using SPR technique and ZnO nanostructured film results in its efficient detection with enhanced sensitivity and low detection limit.

A control experiment was also carried out on gold coated prism by immobilizing the thiolated probe DNA strand on the gold surface (Supplementary Fig. 4). The shift in resonance angle upon probe DNA immobilization and subsequent hybridization with target DNA was found to be much less as compared to that obtained using the ZnO coated gold glass prism. The resonance angle shift after immobilizing probe DNA on bare gold was 1.94°. After DNA hybridization (80 ng/μl), the SPR angle further shifted by 0.84° (Supplementary Fig. 4(a)). However, the corresponding shifts were enhanced significantly in case of ZnO coated gold prism (4.73° and 2.22°) using same concentration of probe and target DNA (Supplementary Fig. 4b). Therefore, the presence of ZnO is important in providing enhanced sensitivity towards meningitis and can be associated with the conformal immobilization of probe DNA and an increased surface reaction area. The porous and nanostructure morphology of ZnO thin film is advantageous for efficient loading of biomolecules and enhanced interactions between the biomolecules and the analyte (Arya et al., 2012).

The specificity studies were also carried out by incubating the ssDNA/ZnO/Au/prism system in a complex sample containing the complementary target as well as two non-complementary DNA strands (Supplementary Fig. 5). On comparison of the data with the curve for only target DNA, it was found that there was no interference with the non-complimentary DNA strands and the shift observed was only due to the target DNA. Hence, the biosensor is highly selective towards *N. meningitidis*. It is important to note that the ssDNA/ZnO/Au/prism can be reused for at least 15 times by denaturation of the hybridized DNA strand without affecting the immobilized DNA probe. This was carried out by immersing the hybridized prism system in hot water for 5 min and subsequent cooling in an ice bath for another 5 min. The obtained SPR curve was found to remain nearly same before and after regeneration confirming the regeneration ability of the ssDNA/ZnO/Au/prism system. After 15 denaturations, the resonance angle was found to shift significantly for the same value of target DNA and the curve could not be retraced. The mean value of shift in the resonance angle (upto 15 denaturations) was found to be 0.37 ± 0.01 for triplicate measurements under similar conditions. The shelf life study of the bioelectrode was carried out at regular intervals of time (every week) for a particular target concentration (80 ng/μl) and the biosensor was found to be stable for more than 12 weeks. There was a continuous minor shift in the resonance angle towards lower side with time, which may be due to the inability of the probe DNA to effectively bind with the target or the desorption of the probe DNA from the ZnO coated gold surface over time.

In order to validate the biosensor, the bioelectrode (ssDNA/ZnO/Au prism system) was incubated separately with two different target-free human blood serum samples and the SPR reflectance curves were recorded. No significant change was observed in the curves. Then, these samples were spiked with the target DNA (80 and 100 ng/μl) and the shift in the SPR curves was compared with the SPR curves for various concentrations of target DNA. The results were found to agree with the corresponding expected values (Supplementary Fig. 6). The measurements were repeated 5 times and the relative standard deviation was found to

be less than 2%. The sensor, thus, displays selectivity, even in complex, clinically relevant blood serum samples.

4. Conclusion

Laboratory assembled surface plasmon resonance (SPR) technique has been successfully exploited for the efficient detection of *N. meningitidis* DNA using ZnO matrix. The developed biosensor exhibits a high sensitivity (0.03°/(ng/μl)), good linearity, low limit of detection (5 ng/μl) and high specificity over a wide concentration range of DNA (10–180 ng/μl). The label free and efficient detection of meningitidis has been demonstrated with good stability, highlighting the encouraging prospects of the prepared SPR biosensor in clinical diagnosis.

Acknowledgments

Authors are thankful to Department of Science and Technology (DST) for the financial support to carry out the proposed work. One of the authors (GK) acknowledges UGC for research fellowship.

Appendix A. Supplementary material

Supplementary data associated with this article can be found in the online version at http://dx.doi.org/10.1016/j.bios.2015.11.025.

References

Arya, S.K., Solanki, P.R., Singh, S.P., Kaneto, K., Pandey, M.K., Datta, M., Malhotra, B. D., 2007. Biosens. Bioelectron. 22, 2516.
Arya, S.K., Saha, S., Ramirez-Vick, J.E., Gupta, V., Bhansali, S., Singh, S.P., 2012. Anal. Chim. Acta 737, 1.
Batra, N., Tomar, M., Jain, P., Gupta, V., 2013. J. Appl. Phys. 114, 124702.
Ben, R.-J., Kung, S., Chang, F.-Y., Lu, J.-J., Feng, N.-H., Hsieh, Y.-D., 2008. J. Formos. Med. Assoc. 107, 448.
Byun, K.M., Kim, N.-H., Ko, Y.H., Yu, J.S., 2011. Sens. Actuators B 155, 375.
Chang, Chia-Chen, Chiu, Nan-Fu, Lin, David Shenhsiung, Chu-Su, Yu, Liang, Yang-Hung, Lin, Chii-Wann, 2010. Anal. Chem. 82, 1207.
Chiba, N., Murayama, S.Y., Morozumi, M., Nakayama, E., Okada, T., Iwata, S., Sunakawa, K., Ubukata, K., 2009. J. Infect. Chemother. 15, 92.
Das, M., Sumana, G., Nagarajan, R., Malhotra, B.D., 2010. Thin Solid Films 519, 1196.
Dash, S.K., Sharma, M., Khare, S., Kumar, A., 2013. Appl. Biochem. Biotechnol. 171, 198.
Dash, S.K., Sharma, M., Kumar, A., Khare, S., Kumar, A., 2014. J. Solid State Electrochem. 18, 2647.
Ghanbari, K., Bathaie, S.Z., Mousavi, M.F., 2008. Biosens. Bioelectron. 23, 1825.
Gupta, V., Mansingh, A., 1996. J. Appl. Phys. 80, 1063.
Homola, J., 2008. Chem. Rev. 108, 462.
Helmerhorst, E., Chandler, D.J., Nussio, M., Mamotte, C.D., 2012. Clin. Biochem. Rev. 33 (4), 161.
Israr, M.Q., Sadaf, J.R., Nur, O., Willander, M., Salman, S., Danielsson, B., 2011. Appl. Phys. Lett. 98, 253705.
Liu, X., Lin, P., Yan, X., Kang, Z., Zhao, Y., Lei, Y., Li, C., Du, H., Zhang, Y., 2013. Sens. Actuators B 176, 22.
Paliwal, A., Tomar, M., Gupta, V., 2014. J. Appl. Phys. 116, 023109.
Patel, M.K., Solanki, P.R., Kumar, A., Khare, S., Gupta, S., Malhotra, B.D., 2010. Biosens. Bioelectron. 25, 2586.
Patel, M.K., Solanki, P.R., Seth, S., Gupta, S., Khare, S., Kumar, A., Malhotra, B.D., 2009. Electrochem. Commun. 11, 969.
Raether, H., 1986. Surface Plasmons on Smooth and Rough Surfaces and on Gratings. Springer Verlag, Berlin.
Schneider, M.C., Exley, R.M., Ram, S., Sim, R.B., Tang, C.M., 2007. Trends Microbiol. 15, 233.
Špringer, T., Homola, J., 2012. Anal. Bioanal. Chem. 404, 2869.
Surinder, K., Bineeta, K., Megha, M., 2007. Indian J. Med. Microbiol. 25, 395.
Tak, M., Gupta, V., Tomar, M., 2014. Biosens. Bioelectron. 59, 200.
Umar, A., Rahman, M.M., Vaseem, M., Hahn, Y.-B., 2009. Electrochem. Commun. 11, 118.
Wang, X., Theodore, M.J., Mair, R., Trujillo-Lopez, E., du Plessis, M., Wolter, N., Baughman, A.L., Hatcher, C., Vuong, J., Lott, L., von Gottberg, A., Sacchi, C., McDonald, J.M., Messonnier, N.E., Mayer, L.W., 2012. J. Clin. Microbiol. 50, 702.
Wang, L., Wang, J., Zhang, S., Sun, Y., Zhu, X., Cao, Y., Wang, X., Zhang, H., Song, D., 2009. Anal. Chim. Acta 653, 109.
Wang, L., Sun, Y., Wang, J., Wang, J., Yu, A., Zhang, H., Song, D., 2010. J. Colloid Interface Sci. 351, 392.
Wood, J.B., Szyndler, M.W., Halpern, A.R., Cho, K., Corn, R.M., 2013. Langmuir 29, 10868.
Zhang, H., Song, D., Gao, S., Zhang, H., Zhang, J., Sun, Y., 2013. Talanta 115, 857.
Zhang, H., Sun, Y., Wang, J., Zhang, J., Zhang, H., Zhou, H., Song, D., 2012. Biosens. Bioelectron. 34, 137.
Zhang, S., Berguiga, L., Elezgaray, J., Roland, T., Faivre-Moskalenko, C., Argoul, F., 2007. Surf. Sci. 601, 5445.
Zhou, X., Nie, H., Yao, Z., Dong, Y., Yang, Z., Huang, S., 2012. Sens. Actuators B 168, 1.
Zhu, H., Wang, Q., Wen, L., Xu, J., Shao, Z., Chen, M., Chen, M., Reeves, P.R., Cao, B., Wang, L., 2012. J. Clin. Microbiol. 50, 46.